COBEM2015

ABCM Associação Brasileira de Engenharia e Ciências Mecânicas

23rd ABCM International Congress of Mechanical Engineering
December 6-11, 2015, Rio de Janeiro, RJ, Brazil

DYNAMIC CHARACTERIZATION AND CONTROL OF A MULTIPURPOSE 3-DOF ASYMMETRIC PARALLEL MECHANISM

Vitor Neves Hartmann
Décio de Moura Rinaldi
Escola Politécnica da USP. Departamento de Engenharia Mecatrônica e de Sistemas Mecânicos. Av. Prof. Mello Moraes, 2231.
vitor.hartmann@usp.br
decio.rinaldi@hotmail.com

Tarcísio Antônio Hess-Coelho
Escola Politécnica da USP. Departamento de Engenharia Mecatrônica e de Sistemas Mecânicos. Av. Prof. Mello Moraes, 2231.
tarchess@usp.br

Abstract. *Parallel kinematic machines have been studied for more than 15 years, with improvements in both structure and control of the mechanism. However, most of its applications were directed to specific tasks of health and industry areas, mainly focusing on workspaces with symmetric dynamic characteristics. There are operations that do not require this condition, namely some pick and place facilities and rehabilitation techniques. A new type of parallel architecture was built within these conditions, and other portability and interchangeability assumptions were made. The prototype's parts are described, and its dynamic properties are briefly compared. Its control is discussed, even though it was not fully implemented, and further studies are being held in order to allow hybrid operation. Position control or force control can be switched, as well as the selection of the number of terms of motion. Control equations are kept in a separate block, independent of data transmission and configuration variables, thus making it possible to change the control law without affecting the rest of the actual assembly, or even allowing the use of different control laws.*

Keywords: *mechanisms, parallel robots, dynamic control*

1. INTRODUCTION

Over the past 15 years there has been a large migration in robotics, from theoretical and experimental developments to applications in sectors other than industry, such as health or home care. Since 2001 the global spending on innovation increased on average about 5% per year. In 2009 and 2010 alone the amount allocated to research in the health area was 22% of that dedicated to industry as a whole, in a total of $ 110 billion and $ 121 billion respectively. In 2011, the three largest companies that invested in research and development were healthcare companies, and the average increase in funding for research and development in these companies was 14% (Jaruzelski *et al.*, 2011).

On the other hand, object manipulation is a characteristic task on some specific sectors, such as electronics, pharmaceutical, food and packaging. Frequently it consists of transferring parts from one production cell to another or between conveyor belts, or even packing final products. For these cases, since the main goal is a high productivity level and the reduction of the cycle times, the energy required to drive the end-effector is reduced due to the low inertia existing in parallel mechanisms, in relation to conventional serial manipulators (Merlet, 2002). Another advantage is the high rigidity that can be achieved once the kinematic chain of the machine is closed (Ceccarelli, 2004).

These two fields share the possibility of using parallel robots with asymmetric distribution of its dynamic characteristics, with benefits in both construction and production (de Almeida and Hess-Coelho, 2010). The tasks that can take benefit from this case are, for instance, the transfer of products between conveyor belts and robot-assisted rehabilitation techniques (de Almeida and Hess-Coelho, 2011). In this context the control of a multi-purpose asymmetric parallel prototype, modular in its construction, with reduced complexity and compatible with the tasks hereby presented is proposed.

2. MATERIALS AND METHODS

The rehabilitation techniques considered were limited to patients with brain stroke, in the flaccid phase or at the beginning of the spastic phase. In the first phase the hemiplegic limb remains flaccid during a period within three weeks and three months, with the condition improving in time. In the second phase the affected limb begins to tremble, or even becomes rigid, for three additional months, a condition that must be treated in order to avoid further progress. The phases considered in this study were simplified and, depending on the author, the quantity of phases varies, with an average of five phases (Steffler, 2007). The periods stated here are also an average, and they vary according to the patient, treatment and time dedicated to the rehabilitation process (da Cunha, 2011).

For those patients the neuromuscular junction, or endplate, is still intact, i.e., capable of receiving and transmitting signals through the nervous system (da Cunha, 2011). For this reason, rehabilitation through repetition is adequate and used as part of the machine rehabilitation software, that changes with increasing difficulty in order to keep the difference between stimulus and response, necessary for the recovery (Weineck, 1991). The parallel system proposed here would then assist other rehabilitation programs, such as the constraint-induced movement therapy, with stronger results in patients with severe upper-limb motor impairment (Finley *et al.*, 2005).

Regarding manipulation, as a general condition, it is preferred that the dynamic characteristics of the workspace are symmetric. However, for the operations listed in this work, systems with asymmetric properties might perform as well as symmetric ones. That is the case for operations with intrinsically different velocities between the orthogonal axes, including rehabilitation: the forces are larger in the anteroposterior direction than in the mediolateral direction, due to the different muscle groups activated and the levers that are created in each situation. Despite being conceived for industrial applications, the lower inertia of the parallel kinematic machines makes them also adequate for physiotherapy in rehabilitation (de Almeida and Hess-Coelho, 2013). Muscle weakness requires that machines intended for this purpose have low impedance and high accelerations, making the parallel kinematic machines more suitable than its serial equivalent (Zollo *et al.*, 2008).

Figure 1 shows the constructed prototype and the parallel machine 3D model. The workspace was designed to allow movements inside a 400mm wide, 400mm long and 100mm high parallelepiped. The interaction force was limited to 20N, with 150W minimum power actuators and maximum weight of the structure of 20kg (Kumazawa *et al.*, 2009). The original 300W power actuators were substituted due to its availability at the time. The hardware used is described as follows: three EPOS2 70/10 controllers, connected through a CAN network, with a single USB connection to the computer; the computer is a 1,83GHz dual processor, with 64bit instructions, 4Gb RAM and USB 2.0 ports; Maxon encoder, planetary gear and electric motor numbers 228456, 203120 and 148867, respectively; three MeanWell power sources model NES-350-27.

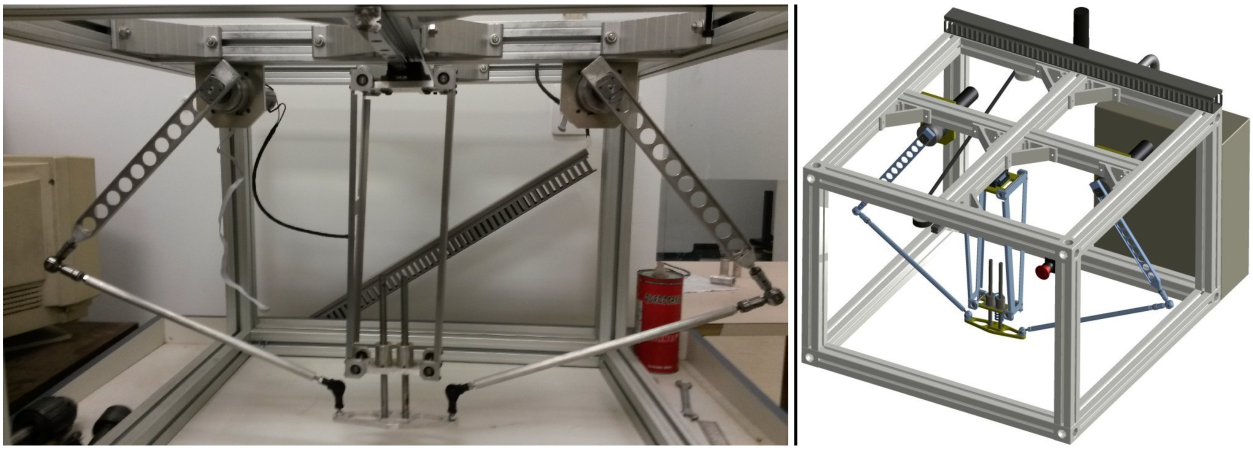

Figure 1. Parallel kinematic machine used in the tests, and its virtual model.

The power consumption of the controllers was estimated in 27,4V already with a safety margin (Maxon, 2013). Considering the power drops due to the wiring, connections and other electronic components, such as buttons, lights and diodes, it was assumed the need for a 30V power source. The power sources selected to work under this condition could provide 11A each without overload. The actuators have a nominal current of 6A and are regulated by the controller. The controller itself will limit the current to 12A due to the motor specifications, and it can hold that condition for less than 13s (estimated through Maxon (2013)).

Within that period of time, all components cannot be damaged: the mechanical transmission is protected by the actuators design; the actuators are protected by the controllers; the controllers and all electric/electronic equipment are protected by the power sources; and the power sources are protected by the circuit breaker. All the structure and its equipment are properly grounded, and the machine was designed to work at full capacity with regular high current AC power supply sockets (in this particular case, 20A standard).

The accuracy and the repeatability were calculated based on the ANSI (1990) and the MSA (2010). The accuracy is presented as the percentage error between each measured value and the theoretical position given to the machine. The repeatability is presented as the percentage error between each measured value and their respective calculated average. In both cases the deviation is represented by the standard deviation of the errors, again as a percentage. The plotted graphics show the mean and standard deviation of the calculated errors, and they were approximated by using a fourth degree polynomial, as it was an expected behavior according to the used equations.

The coordinate system was placed according to Fig. 2: the origin is fixed at the center of the line segment connecting the two actuators shafts. The X axis is oriented perpendicular to that distance and parallel to the horizontal plane. The Y axis comprehends the two actuators shafts and is perpendicular to each of them, thus parallel to the horizontal plane. The Z axis is perpendicular to the horizontal plane, starting at the origin and oriented downwards. The orientation of the X and Y axes is given by the right-hand rule. Since the current working mechanism is planar on (0,Y,Z), three vertical levels were selected for the measurements: the highest one at 370mm, limited by construction; the lowest one at 430mm, limited only by the capability of acquiring data with the measuring system; and an intermediate position at 400mm.

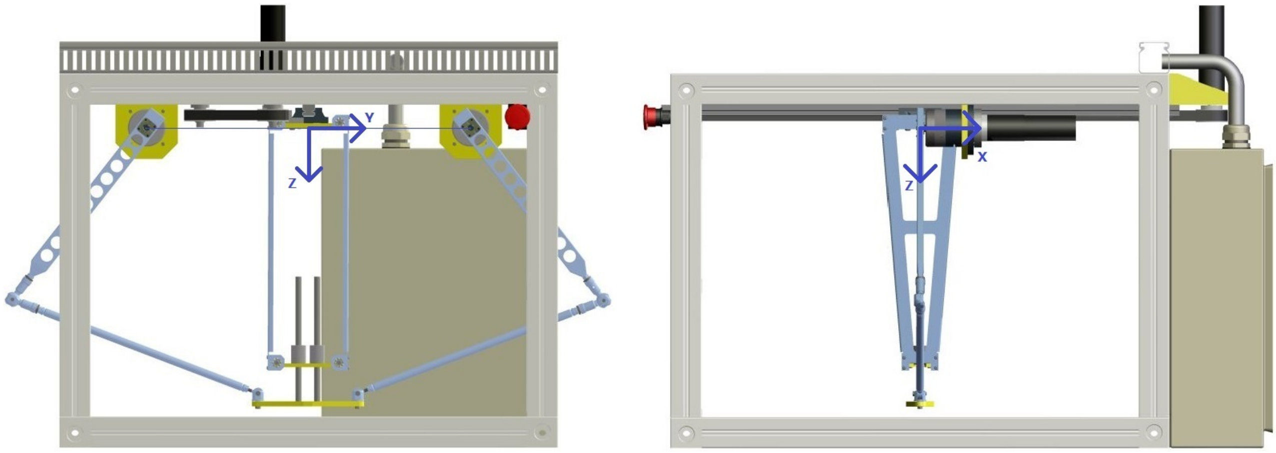

Figure 2. Origin location: front view and right lateral view, respectively.

At each level, the Y distance was varied in 10mm steps, equally distributed in the positive and negative values of the axis, in a total of 25 points, including the origin. Each point was measured 20 times along the Y direction, half of them starting from the origin, and the other half starting from the extremity of $\pm$120mm. Thus, each level has a total of 500 measurements, corresponding to 1500 acquired values in this experiment. At each desired position the results of the measuring system were transferred to an acquisition and post processing program written in Matlab. The dataflow of the main components used is shown in Fig. 3.

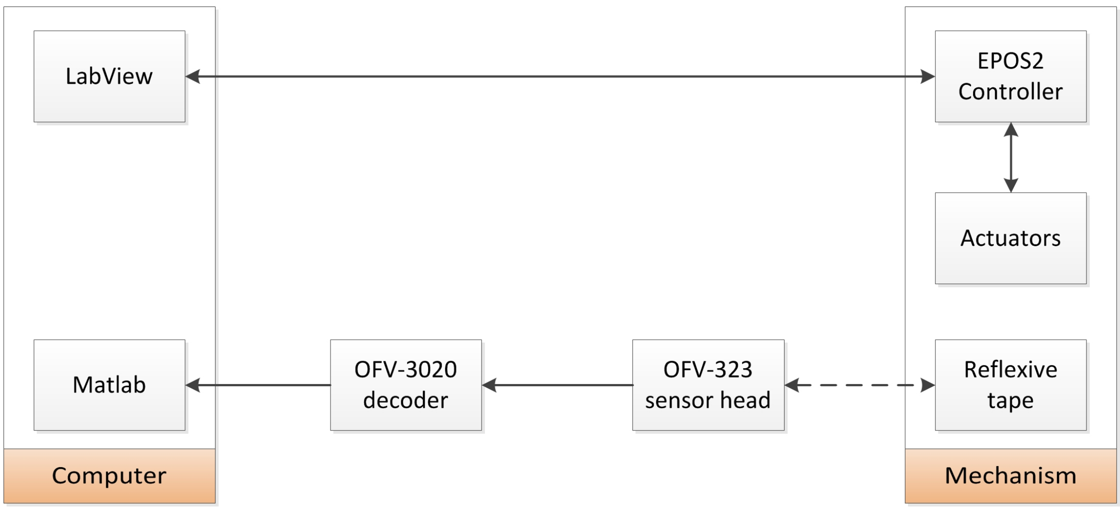

Figure 3. Simplified system dataflow.

The measuring system used was a Polytec laser Doppler vibrometer composed of a OFV-323 sensor head and a OFV-3020 decoder. The experiment mounting was according to Fig. 4. The displacement output of the decoder was operated with a scaling factor of 10.240μm and frequency lower than 50Hz. The maximum displacement registered in that condition is 80mm, but it was limited to 60mm in order to reduce measurement errors. Resolution is 40μm and the amplitude error was above 1% due to the lower frequency. The sensor head was a helium neon laser type running at 80MHz and with a stand-off distance of 450mm. Transport, storage, warm-up and other operating and maintenance requirements were respected.

At the present, trials are being performed on the velocity control of the trajectory but, until the completion of the tests cited in this article, the desired path was achieved only through a positioning control based on inverse kinematics. The kinematic diagram of the parallel machine constructed is shown in Fig. 5.

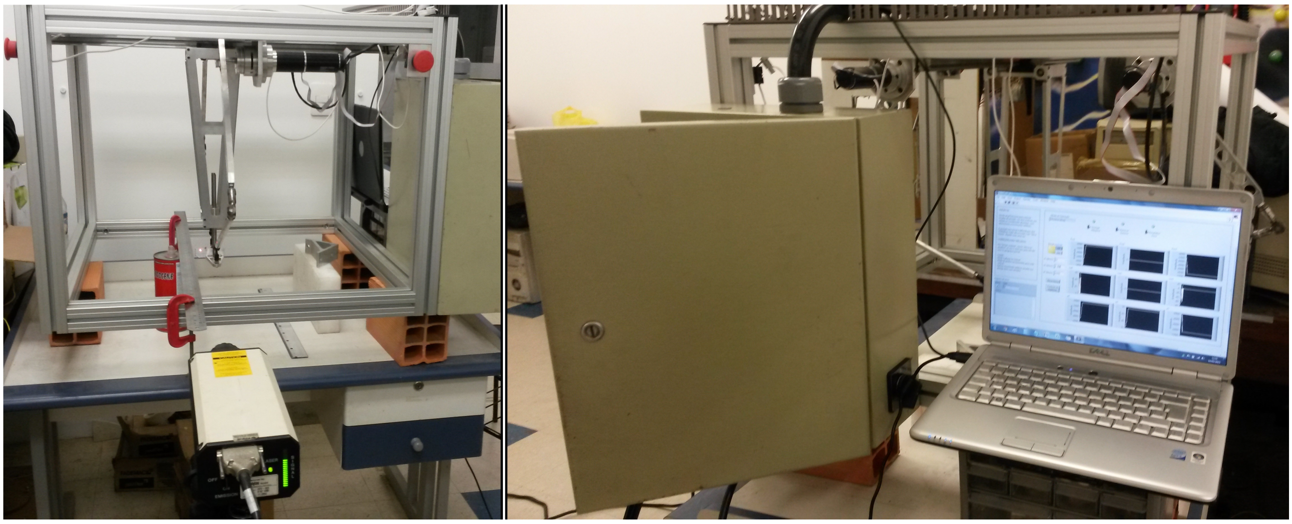

Figure 4. Measuring system, computer and front panel of the developed program.

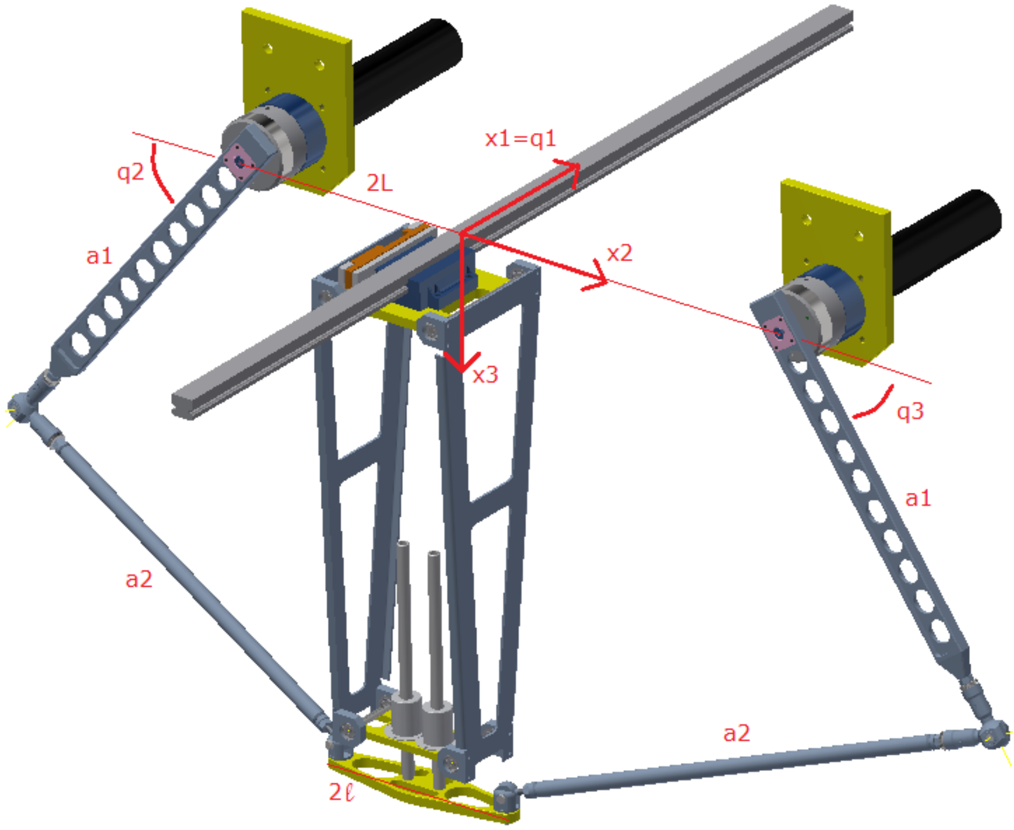

Figure 5. Kinematic diagram of the built machine.

Through geometry it is possible to establish links between the end-effector and the actuators coordinates, as shown in Eq. (1), Eq. (2) and Eq. (3).

$$x_1 - q_1 = 0 \tag{1}$$

$$x_1^2 + (x_2 - l + L + a_1 \cdot \cos(q_2))^2 + (x_3 - a_1 \cdot \sin(q_2))^2 - a_2^2 = 0 \tag{2}$$

$$x_1^2 + (x_2 + l - L - a_1 \cdot \cos(q_3))^2 + (x_3 - a_1 \cdot \sin(q_3))^2 - a_2^2 = 0 \tag{3}$$

It is possible to isolate the actuators coordinates to obtain the inverse kinematics. Equation (4), Eq. (5) and Eq. (6) show the relations used to control the position of the end-effector. Note that the system is partially decoupled and, thus, easier to resolve.

$$q_1 = x_1 \tag{4}$$

$$q_2 = 2 \cdot \arctan\left(\frac{-k_{21} \pm \sqrt{k_{21}^2 + k_{22}^2 - k_{23}^2}}{k_{23} - k_{22}}\right) \quad (5)$$

$$q_3 = 2 \cdot \arctan\left(\frac{-k_{31} \pm \sqrt{k_{31}^2 + k_{32}^2 - k_{33}^2}}{k_{33} - k_{32}}\right) \quad (6)$$

Where:

$$k_{21} = -2 \cdot x_3 \cdot a_1 \quad (7)$$

$$k_{22} = 2 \cdot (x_2 - l + L) \cdot a_1 \quad (8)$$

$$k_{23} = x_1^2 + (x_2 - l + L)^2 + x_3^2 + a_1^2 - a_2^2 \quad (9)$$

$$k_{31} = -2 \cdot x_3 \cdot a_1 \quad (10)$$

$$k_{32} = -2 \cdot (x_2 + l - L) \cdot a_1 \quad (11)$$

$$k_{33} = x_1^2 + (x_2 + l - L)^2 + x_3^2 + a_1^2 - a_2^2 \quad (12)$$

One can note that there are four independent solutions for each q_2 and q_3. However, in practice, there are only two since the function $\arctan$ provides the same result for angles located in the second and third quadrants. The two remaining solutions can be filtered by limiting q_2 and q_3 from 0 to 90 degrees, due to its construction. Thus, it is desired only the solution located at the first quadrant of the unit circle. Further details on the equating can be found at de Almeida (2013).

The block diagram that represents the information flow of the desired position is shown in Fig. 6. The PID gains $K_p = 709$, $K_i = 2219$ and $K_d = 1209$ were obtained through the auto tuning function provided by the manufacturer of the motors. Since the final objective is to operate the machine using the Computed Torque Control, the function was a good starting point to be used with the position control. Once the Computed Torque Control is implemented, further manual tuning will be necessary for optimal regulation of the parameters.

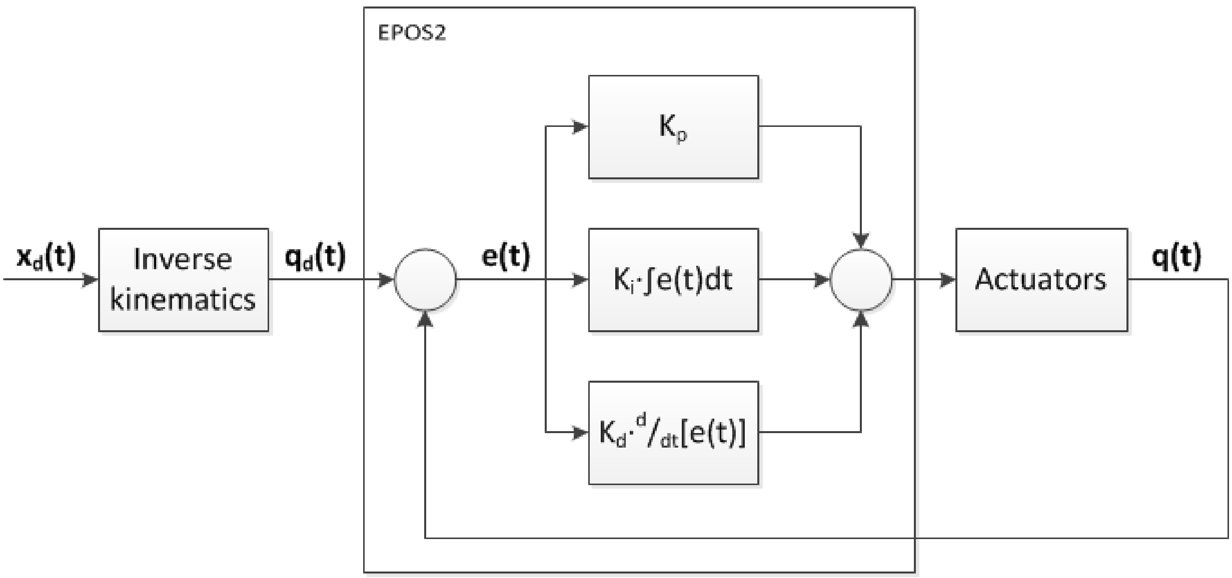

Figure 6. Block diagram of the positioning controller.

The controller was instructed using a program developed in LabVIEW, version 2012, SP1, 32bits. The program has a central structure called Formula Node into which the control law is written with mathematical formulas and expressions similar to C. This allows that the type of control is changed according to the desired needs and that, as it will be shown, other types of control are implemented in the future.

3. RESULTS

The measured results were treated and are presented as follows. As stated, the accuracy was calculated as a percentage error between each measured value and the theoretical desired position, and is shown in Fig. 7. Likewise, the repeatability was calculated as a percentage error between each measured value and their respective average, and is shown in Fig. 8.

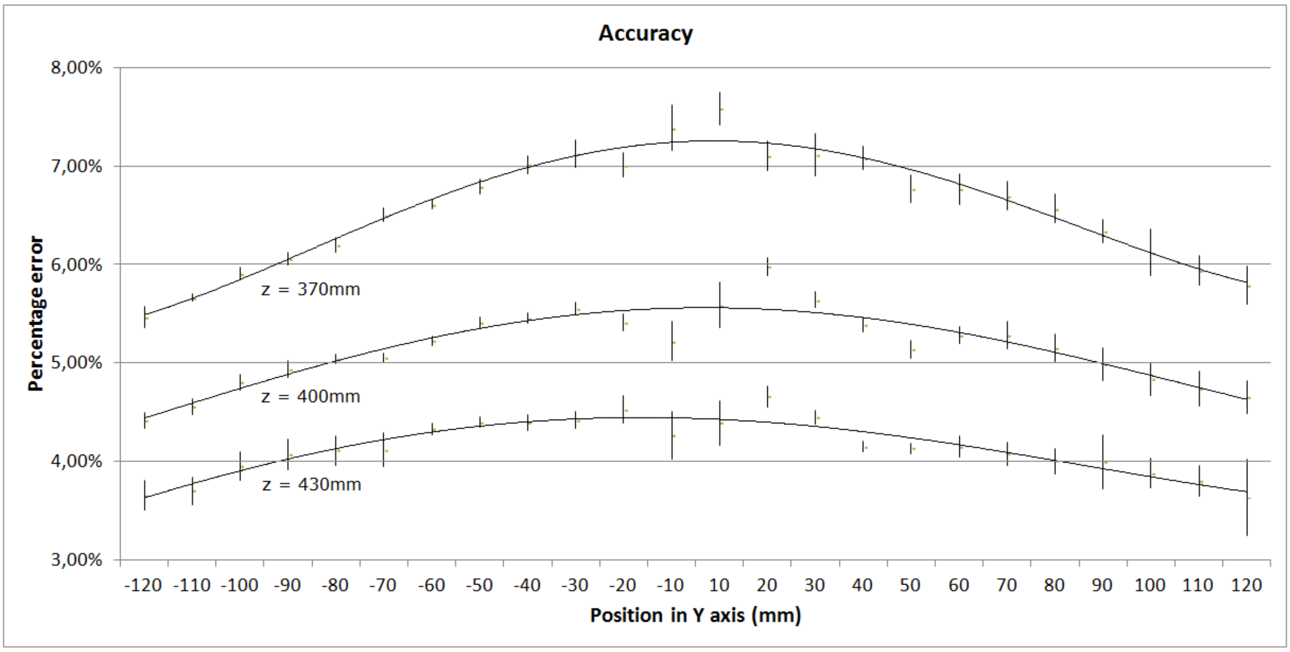

Figure 7. Percentage error in relation to the theoretical values at three different levels.

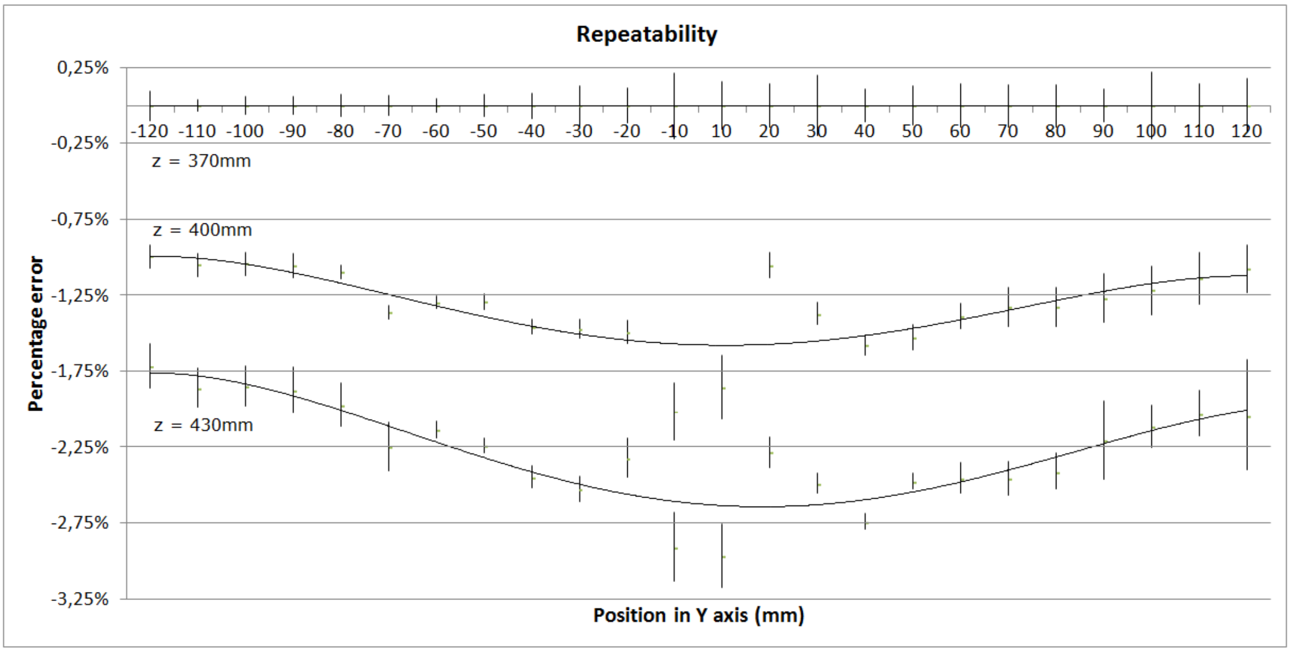

Figure 8. Percentage error in relation to the mean of the values at three different levels.

The three levels are present in both graphics by means of a dot and a vertical bar representing the average and the standard deviation of the measured data, respectively.

It is possible to see in Fig. 7 that the accuracy improves as the end-effector moves away from the origin along the Z axis. The polynomial chosen seem to depict the behavior of the data except in the vicinity of the Z axis. It is also noticed that the positive positions in the Y axis are slightly less accurate than the respective negative positions, and the former also applies to the standard deviation of the error. The module of the maximum and minimum approximate values of the accuracy errors at the observed points are, respectively, 7,6% and 3,6%.

Figure 8 shows that the repeatability improves as the end-effector moves towards the origin along the Z axis. The polynomial chosen seem to depict the behavior of the data except in the vicinity of the Z axis. It is also noticed that the positive positions in the Y axis are slightly less accurate than the respective negative positions, and the former also applies to the standard deviation of the error. The module of the maximum and minimum approximate values of the repeatability errors at the observed points are, respectively, less than 0,1% and 3%.

4. DISCUSSION

The results observed in Fig. 7 at first did not seem to be coherent with the expected behavior. However, after carefully analyzing the prototype built and the existing forces acting at the selected positions, it was discovered that they in fact might be. The machine as it is has considerable clearances at the joints connecting the limbs, which in turn, when in the vicinity of the Z axis, are directed in opposite symmetry by the actuators. In this situation the slightest disturbance of the system could alter the position of the end-effector in the Y axis. On the other hand, as one moves away from the Z axis, all the clearances are directed to the same side, and the own weight of the articulated parallelogram contributes to render the structure more rigid.

As one moves to Fig. 8 it is possible to see the previous hypothesis occurring again. In the vicinity of the Z axis the repeatability also decreases; after moving to the extremities of the targeted area in the Y direction the system becomes more reliable. Also, by approaching the end-effector to the articulated parallelogram the clearances of the prismatic joint have less effect on the errors, a situation that is reversed after increasing the distance from the origin. Overall, there is a need to further reduce the clearances of the parallel prototype built, since they still seem to be influencing the position of the end-effector in an undesirable way.

It was also observed that the measuring system affects the results. It is well known that this often occurs, but the results change noticeably over the chosen path. After some observation, it is suggested that both the calibration and the type of the signal could be the cause of such variations. To determine if the first cause is in fact true, the condition of the laser will be tested against a local coordinate machine, to verify if the measured data need correction. The second cause can be analyzed by changing the displacement measurement signal into the velocity measurement signal.

The problem arises from hardware limitation in the measuring system: the internal integrator is limited by the scaling factor of 10.240μm and the voltage range of 16V peak-peak, leading to the 80mm measuring limit (160mm full scale). And since the frequency is low, there is an increase in accumulated errors that could be responsible for the variation in the data. By using the velocity signal with a scaling factor of 10mm/s, and considering that the voltage range in this case is of 20V peak-peak, the measuring limit becomes 100mm/s (200mm/s full scale) with a resolution of 1,2μm/s, more than enough for the considered purpose. The signal could be later integrated inside the computer, eliminating the need of constantly clearing the measuring system and possibly reducing the measurement errors.

As mentioned previously, it is desired that the type of control is changed according to the tasks performed. Presently, besides the position control, trials are being carried out on the velocity control in order to allow a smooth control of the trajectory. One future idea is to control this system not with a position control, but based on the Computed Torque Control, as briefly explained in the following paragraphs.

In that case there would be two major problems: the first one is the discrete nature of the computer calculations that introduce errors considering the continuous time characteristic of these equations; the second one is that the model used is not exactly representative of the real behavior, generating more errors.

Both could be circumvented: the sampling rate of the EPOS2 controller is 10kHz, which highly exceeds the frequency of the considered phenomena. Moreover, the computer used is supposed sufficient for the real time control, and the equations could be simplified in order to consider only the terms with more than 5% of participation in the total value of the torques, without considerable errors (de Almeida and Hess-Coelho, 2013).

For pick and place activities, the difference between the model and the real behavior could be minimized through a PID controller. In the case of rehabilitation tasks, since precision is not that necessary, a simpler PD controller will be used. The main equation is given in Eq. (13), where τ is the torque applied by the actuators, α is the mass matrix, β contains gravity terms amongst others, and τ' contains the controller's constants K_v, K_p and K_i correcting the position errors E and the velocity errors $\dot{E}$.

$$\tau = \alpha\tau' + \beta \tag{13}$$

Where:

$$\alpha = I \tag{14}$$

$$\beta = G(\phi) \tag{15}$$

$$\tau' = \phi_d' + K_v \cdot \dot{E} + K_p \cdot E + K_i \cdot \int E\mathrm{d}t \tag{16}$$

Disturbances could be considered in order to include the dynamic of the affected limb. These were classified into two types of disturbance: unit steps within the trajectory, representing throes, and sinusoidal waves, representing the tremors. The first ones are assumed to have a 0,1m peak, and the second ones 0,05m amplitude and 5Hz frequency (Borges and Ferraz, 2006). The frequency range can be considered to be between 0,01Hz and 10Hz, and forces magnitudes are between 0,1N and 100N, with a typical value of 10N (Ju *et al.*, 2005).

Further details on the Computed Torque Control equations will be presented in future works, as well as the adopted gains.

5. CONCLUSION

In this work it was shown that for some operations machine workspaces have no need to present symmetric dynamic characteristics. A new type of parallel architecture was built with these technical features and tested using a position control. Its accuracy and repeatability were calculated by measuring the errors in relation to the theoretical position and the calculated average at each point, respectively. Despite all the previously mentioned problems, the results show that the proposed architecture is feasible, and that, after some additional analysis over the measuring system and the prototype itself, some adjustments need to be done in order to improve those results.

6. ACKNOWLEDGEMENTS

Igor Neves Hartmann, for the revision of this article.
Rafael Traldi Moura, for providing the laser measuring system and the acquisition software.
Brian Juan Auza Tarquino, for briefing the acquisition software.

7. REFERENCES

ANSI, 1990. "Ansi/ria r15.05-1-1990 - point-to-point and static performance characteristics - evaluation".
Borges, V. and Ferraz, H.B., 2006. "Tremores". *Revista Neurociências*, Vol. 14, No. 1, pp. 43 – 47.
Ceccarelli, M., 2004. *Fundamentals of mechanics of robotic manipulation*. Dordrecht: Kluwer.
da Cunha, C., 2011. *Introdução à Neurociência*. Editora Átomo.
de Almeida, R.Z.H., 2013. *Modelagem dinâmica e controle de robô manipulador de arquitetura paralela assimétrica de três graus de liberdade*. Ph.D. thesis, Escola Politécnica da Universidade de São Paulo.
de Almeida, R.Z.H. and Hess-Coelho, T.A., 2010. "Dynamic model of a 3-DOF asymmetric parallel mechanism". *The Open Mechanical Engineering Journal*, , No. 4, pp. 48–55.
de Almeida, R.Z.H. and Hess-Coelho, T.A., 2011. "Structural synthesis, dynamic modeling and analysis of a 3-DOF asymmetric parallel mechanism". *Journal of Mechanics Engineering and Automation*, , No. 1, pp. 481–490.
de Almeida, R.Z.H. and Hess-Coelho, T.A., 2013. "Dynamic model simplification of an asymmetric parallel robot for the development of real time control system". *Proceedings of the XV International Symposium on Dynamic Problems of Mechanics*.
Finley, M.A., Fasoli, S.E., Dipietro, L., Ohlhoff, J., MacClellan, L., Meister, C., Whitall, J., Macko, R., Jr, C.T.B., Krebs, H.I. and Hogan, N., 2005. "Short-duration robotic therapy in stroke patients with severe upper-limb motor impairment". *Journal of Rehabilitation Research and Development*, Vol. 42, No. 5, p. 683 to 692.
Jaruzelski, B., Loehr, J. and Holman, R., 2011. "Why culture is key". *strategy+business*.
Ju, M.S., Lin, C.C.K., Lin, D.H., Hwang, I.S. and Chen, S.M., 2005. "A rehabilitation robot with force-position hybrid fuzzy controller: Hybrid fuzzy control of rehabilitation robot". *IEEE Transactions on Neural Systems and Rehabilitation Engineering*, Vol. 13, No. 3, pp. 349 – 358.
Kumazawa, V.D., Hess-Coelho, T.A., Rinaldi, D., Carbone, G. and Ceccarelli, M., 2009. "Kinematic analysis and operation feasibility of a 3-DOF asymmetric parallel mechanism". In *Proceedings of COBEM 2009*.
Maxon, 2013. *EPOS2 Positioning Controller: Hardware Reference*. Maxon Motor Control, april 2013 edition.
Merlet, J.P., 2002. "Still a long way to go on the road for parallel mechanism". In *ASME DETC Conference*.
MSA, 2010. *Measurement Systems Analysis*, 4th edition.
Steffler, K., 2007. "Reabilitação do paciente com avc". Escola de Massoterapia SOGAB.
Weineck, J., 1991. *Biologia do Esporte*. Editora Manole Ltda.
Zollo, L., Accoto, D., orchiani, F.T., Formica, D. and Guglielmelli, E., 2008. "Design of a planar robotic machine for neuro-rehabilitation". *IEEE International Conference on Robotics and Automation*.

8. RESPONSIBILITY NOTICE